Communication: Hot-atom abstraction dynamics of hydrogen from tungsten surfaces: The role of surface structure

Oihana Galparsoro, Heriberto Fabio Busnengo, Joseba Iñaki Juaristi, Cédric Crespos, Maite Alducin, and Pascal Larregaray

Citation: The Journal of Chemical Physics **147**, 121103 (2017); doi: 10.1063/1.4997127
View online: http://dx.doi.org/10.1063/1.4997127
View Table of Contents: http://aip.scitation.org/toc/jcp/147/12
Published by the American Institute of Physics

Communication: Hot-atom abstraction dynamics of hydrogen from tungsten surfaces: The role of surface structure

Oihana Galparsoro,[1,2,3] Heriberto Fabio Busnengo,[4] Joseba Iñaki Juaristi,[3,5,6] Cédric Crespos,[1,2] Maite Alducin,[3,6] and Pascal Larregaray[1,2,a)]
[1]*CNRS, ISM, UMR5255, F-33400 Talence, France*
[2]*Univ. Bordeaux, ISM, UMR5255, F-33400 Talence, France*
[3]*Donostia International Physics Center (DIPC), Paseo Manuel de Lardizabal 4, 20018 Donostia-San Sebastián, Spain*
[4]*Instituto de Física Rosario (IFIR) CONICET-UNR, Esmeralda y Ocampo, 2000 Rosario, Argentina*
[5]*Departamento de Física de Materiales, Facultad de Químicas (UPV/EHU), Apartado 1072, 20080 Donostia-San Sebastián, Spain*
[6]*Centro de Física de Materiales CFM/MPC (CSIC-UPV/EHU), Paseo Manuel de Lardizabal 5, 20018 Donostia-San Sebastián, Spain*

(Received 21 July 2017; accepted 14 September 2017; published online 29 September 2017)

Adiabatic and non-adiabatic quasiclassical molecular dynamics simulations are performed to investigate the role of the crystal face on hot-atom abstraction of H adsorbates by H scattering from covered W(100) and W(110). On both cases, hyperthermal diffusion is strongly affected by the energy dissipated into electron-hole pair excitations. As a result, the hot-atom abstraction is highly reduced in favor of adsorption at low incidence energy and low coverages, i.e., when the mean free path of the hyperthermal H is typically larger. Qualitatively, this reduction is rather similar on both surfaces, despite at such initial conditions, the abstraction process involves more subsurface penetration on W(100) than on W(110). *Published by AIP Publishing.* https://doi.org/10.1063/1.4997127

Surface properties are known to largely influence the kinetics and dynamics of elementary gas-solid heterogeneous processes.[1,2] In particular, surface structure significantly affects adsorption, dissociative chemisorption, and recombination processes. As prototypical examples from catalysis, the dissociation probability of N_2 molecules over iron varies by order of magnitudes, decreasing from (111) to (100) and (110) crystal faces at low gas pressure.[3] Simulations of molecular beam experiments on Fe(111)[4] and Fe(110)[5,6] also exhibit this trend for N_2 adsorption. Large effects are also experimentally and theoretically observed in the initial sticking probability of N_2 on tungsten surfaces[7–10] and O_2 on the three low-index crystal faces of silver.[11–17] Molecular recombination is also affected by the crystal face as revealed, for instance, by the experiments on hydrogen formation at metals carried out by Küppers *et al.*[18–25] and Winkler *et al.*[26–29] The observed kinetics for H(D)+D(H)/metal recombination has been rationalized via models that required a significant variation of the rate constants for H_2, HD, and D_2 formations for the three low-index faces of Pt[19–22] and also for Cu(111) and Cu(100).[23,24]

On the sub-picosecond time scale, recombinations proceed via Eley-Rideal (ER) or Hot-Atom (HA) abstractions. The former mechanism involves direct collision between a scattering atom (projectile) and an adsorbed species (target),[30] while the latter is governed by hyperthermal diffusion of the projectile onto the surface prior to abstraction.[31]

The influence of the crystal face has been recently scrutinized theoretically for the Eley-Rideal (ER) recombination of hydrogen and nitrogen on the W(100) and W(110) surfaces,[32–36] accounting for dissipation to surface phonons and electrons.[37] In these direct ultrafast processes, the surface is thought to mostly behave as a spectator. Nevertheless, significant differences in the abstraction mechanisms and cross sections have been predicted, stemming from the distinct topologies of the interactions upon approach of the projectile towards the target. Regarding N_2 ER abstraction, a repulsive potential energy structure, involving strong corrugation in the entrance channel, is responsible for a 0.53 eV threshold for abstraction from W(100). Such a structure is much smaller and less extended on W(110) and consequently affects much less ER reactivity as a function of the incidence energy.[32–34] H_2 ER abstraction on tungsten also reveals distinct recombination mechanisms depending on the surface structure. On W(110), recombination occurs after rebound of the projectile on the W surface atoms in the close vicinity of the target. Conversely, a significant fraction of recombination takes place after rebound of the projectile on second layer W atoms for W(100).[35] Energy dissipation to the metal has been predicted to be mainly mediated by phonon excitations for nitrogen and by low-energy electron-hole *(e–h)* pairs for hydrogen. Dissipation has been found to quantitatively affect N_2 reactivity but only marginally that of H_2.[37]

Though extended knowledge has been gathered on ER abstraction, pioneering molecular dynamics simulations[38–40] and comparisons between kinetics experiments and models[18,38,41,42] have suggested hydrogen abstraction to essentially proceed via the HA process for various metals. Recent theoretical works have thus focused on this issue, in particular for H_2 recombining from W(110).[43,44] Interestingly, it was

a)pascal.larregaray@u-bordeaux.fr

predicted that, if hot-atom abstraction dominates recombination at low coverage when neglecting possible energy dissipation to the metal (adiabatic approximation), this process is importantly reduced in favor of adsorption as soon as dissipation to the surface[44] or to preadsorbed species[43] is significant. For hydrogen atoms and molecules interacting with metallic surfaces at low coverage, for which collisions with pre-adsorbed species are unlikely, the main energy dissipation channel in the picosecond time scale is the excitation of low lying *e–h* pairs.[45–52] As such an effect depends on the surface electronic structure, its sensitivity to the crystal face is a relevant issue that we address in the present study. To this end, we compare, in the following, the dynamics of H_2 formation by abstraction of pre-adsorbed H atoms upon H atom scattering at finite coverage for the W(100) and W(110) surfaces.

The normal incidence scattering of atomic hydrogen off H-covered W(100) and W(110) surfaces is simulated via quasiclassical trajectories (QCT), which initially account for the adsorbates zero point energy (ZPE), for, respectively, Θ = 0.5 ML and 0.25 ML coverages. Note that in selecting these coverages, the surface area per adsorbate is similar, $\approx$20.1 Å^2 and $\approx$28.4 Å^2, respectively. Related multiadsorbate potential energy surfaces (PESs), which rely on density functional theory (DFT) calculations, were developed[43,53] as an expansion up to two H-terms[39,40] of a diatom-surface interpolated PES, derived from an adaptation of the corrugation reducing procedure (CRP).[54–56]

QCT calculations use a 6 × 6 supercell with periodic boundary conditions in order to model an infinite covered surface. The surface unit cell is a $(a \times a)$ square for W(100) while it is a $(a \times a\sqrt{2})$ rectangle for W(110) as sketched in Fig. 1 (a = 3.17 Å). For both surfaces, the classical equations of motion are integrated for one projectile atom and 18 adsorbed targets with initial positions and velocities given by the ZPE as detailed in previous studies.[35,36] The initial altitude of the projectile is taken in the asymptotic region of the potential, at Z_p = 7.0 Å from the surface. The (X_p, Y_p) initial position of the projectile is randomly sampled in the covered surface irreducible cell (yellow areas of Fig. 1). To ensure convergence, respectively, 30 000 and 120 000 trajectories have been computed for W(100) and W(110). Since the multiadsorbate PESs ignore possible interaction between three hydrogen atoms,[43,53]

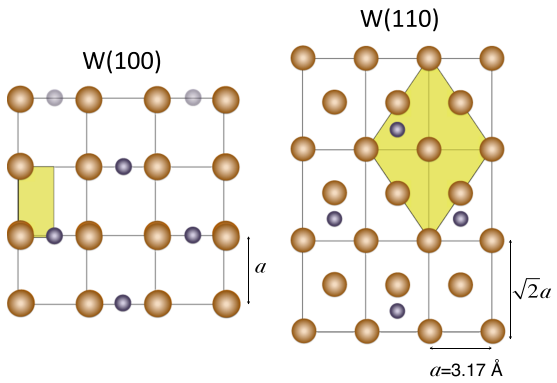

FIG. 1. Position of the adsorbed H atoms (purple points) at Θ = 0.5 ML for W(100) (left) and Θ = 0.25 ML for W(110) (right). The lattice constant parameter is a = 3.17 Å. Sampling areas of initial (X_p, Y_p) positions of the projectiles for each coverage are represented in yellow.

trajectories are stopped whenever one H atom has two neighbouring H atoms closer than 1.5 Å. Since the actual fate of such trajectories is unknown, the corresponding contribution is taken as an uncertainty to any possible outcome of scattering.[35,36,43] The vibration of the formed H_2 molecules has been semiclassically quantized via the Gaussian weighting procedure.[57–59]

In order to rationalize nonadiabatic effects upon scattering, molecular dynamics simulations are performed within the Born-Oppenheimer static surface (BOSS) approximation and within the local density friction approximation (LDFA).[60] In the former case, neither energy exchange with the surface phonons nor electronic excitations are accounted for. In the latter, electronic nonadiabaticity is introduced through a dissipative force in the classical equations of motion for the hydrogen atoms. This approach has already been used to investigate non-adiabatic effects in gas-surface elementary processes[46,48–51,61–63] and allows a good compromise between accuracy and simplicity.[51,64] The friction force, acting independently on each H atom, is approximated as the one corresponding to a homogeneous free electron gas with electronic density equal to that of the bare surface at the atom position. This approximation has been recently used to rationalize the adsorption and relaxation of H, N, and N_2 on bare metallic surfaces,[46,48,50] as well as for recombinative H_2 desorption induced by fs-laser pulses.[65,66] Dissipation to surface phonons is neglected here as dissipation to electrons has been recently predicted to largely dominate the relaxation of hydrogen on metals in the sub-picosecond time scale.[45–48]

As a result of H-atom scattering, recombination may occur via three different processes: ER abstraction is assumed when the formed molecule moves definitively toward the vacuum after the first rebound of the projectile.[37] Otherwise, abstraction is considered as primary HA process. Whenever abstraction involves two target atoms, it is classified as a secondary HA process.[67] If not reactive, H-scattering may lead to reflection, whenever one atom reaches the initial altitude of the projectile, absorption, if one atom lies below the surface (Z < 0 Å) after the 1 ps total integration time, and otherwise, adsorption.

The recombination cross sections *per* adsorbate are displayed in Fig. 2 as a function of the incidence energy of the projectile, E_i, for both W(110) (top panels) and W(100) (bottom panels) surfaces. The left panels correspond to results within the BOSS approximation, whereas the right ones account for dissipation to *e–h* pairs within the LDFA. When neglecting energy dissipation, primary HA abstraction dominates at low incidence energies. This channel is more reactive on W(110) for which the density of adsorbates is lower [0.035 ad./Å^2 for W(110) vs. 0.05 ad./Å^2 for W(100)]. This result originates from the lower probability of adsorption mediated by energy dissipation to H-preadsorbed atoms, which has been previously shown to be a very efficient process.[43,44] Secondary HA abstraction is accordingly also more efficient on W(110). As observed in the single adsorbate limit,[35,37] ER abstraction proceeds, on the W(100) surface, via collision of the projectiles not only with neighbouring W surface atoms on the top most layer but also with second layer W atoms. A similar difference between the two surfaces is observed in the

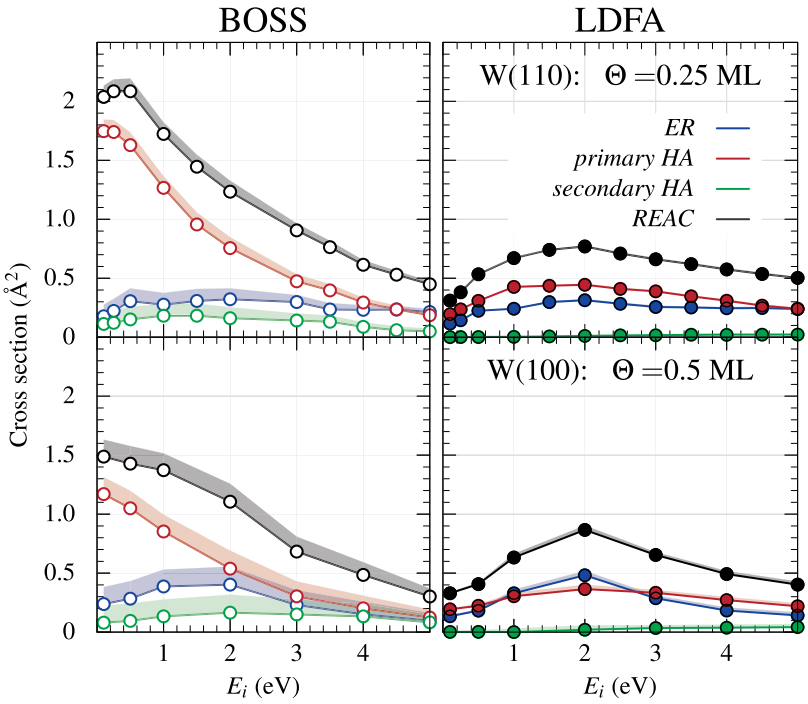

FIG. 2. Cross sections *per* adsorbate for ER (blue), primary HA (red), secondary HA (green), and total (black) abstraction as a function of E_i. Left (right) panels correspond to BOSS (LDFA) results. Top (bottom) panels correspond to W(110) [W(100)]. Uncertainties, which correspond to the contribution of stopped trajectories (see text), are represented by shaded domains when their contribution is larger than the size of the symbols.

HA recombination process. Upon increasing incidence energy, abstraction reactions are reduced because hot atom formation, which requires the transfer of incidence energy from normal to parallel motions with respect to the surface, becomes less and less probable at the expense of projectile reflection.[43,44] At the highest energies studied, primary HA and ER are of comparable reactivity on both surfaces.

When including *e–h* pair excitations (right panels), a strong decrease of the primary HA abstraction is predicted below 2 eV incidence energy for both W(100) and W(110). Besides, secondary HA recombination is also greatly affected over the whole range of incidence energy studied. The absolute abstraction cross sections are significantly lower than the ones suggested from the comparison between kinetics experiments and models[18,38,41,42] for other metals. However, such a comparison is not straightforward and a specific experiment to measure sub-picosecond abstraction absolute cross sections would be needed.

As previously analyzed,[44] the significant reduction of the cross sections originates from the high efficiency of electronic excitations in cooling down hot projectiles during hyperthermal diffusion onto the surface to lead to adsorption. This is highlighted in Fig. 3 in which E_p, i.e., the total energy distribution of the projectile, is displayed as a function of time for $E_i = 0.5$ eV for both the BOSS and LDFA calculations. The origin of energies is here taken for the adsorbate in its equilibrium position and the projectile in the gas phase. For both surfaces, the time evolution of the projectile total energy distribution is rather similar. The abstraction process is exothermic by about 1.5 eV for both systems, and it becomes energetically closed when the total energy of the projectile is below −1.5 eV. The latter occurs much faster when accounting for energy dissipation to *e–h* pairs for which almost all the projectiles have lost the available energy for reaction in about 0.25 ps within the LDFA (black), while only half of them have done it within the BOSS approximation (red). The similarity for the energy loss to *e–h* excitations between both surfaces is striking in view of the different abstraction dynamics that we have identified.

For W(100), 34% of the reactive collisions involve a rebound below the surface level, where coupling to the surface electrons is expected to be stronger, while less than 4% do so for the W(110). However, a detailed analysis of the abstraction dynamics actually shows that on average the recombining projectiles probe regions of larger electron density on the closer packet W(110) surface. these differences are small nevertheless and hardly affect the energy loss to the metal, since other factors such as the interaction time and projectile velocity come into play that compensate for the slightly stronger coupling in the W(110) surface. In the end, the predicted final energy loss and non-adiabatic effects in the cross section appear to be quite independent of the surface plane.

As a consequence of the energy loss, the distance travelled by the projectile on the surface is considerably affected as illustrated in Fig. 4. This figure shows the BOSS and LDFA results for the normalized travelled distance distribution for abstraction (HA + ER) from the W(100) and W(110) surfaces at 0.5 eV incidence energy. Hyperthermal diffusion distances are significantly reduced when accounting for energy dissipation into *e–h* pair excitations. Actually, the abstracted adsorbates are mostly the ones initially located in the irreducible surface unit cell or the neighboring ones. The reduction of the projectile travelled length caused by *e–h* pair excitations is also the reason of the strong decrease observed in the LDFA secondary HA reactivity.

As a result of abstraction, energy is mainly channeled into translation of the formed molecule for both surfaces. The average internal energy and its partition between rotation and vibration do not significantly depend on surface structure (not shown).

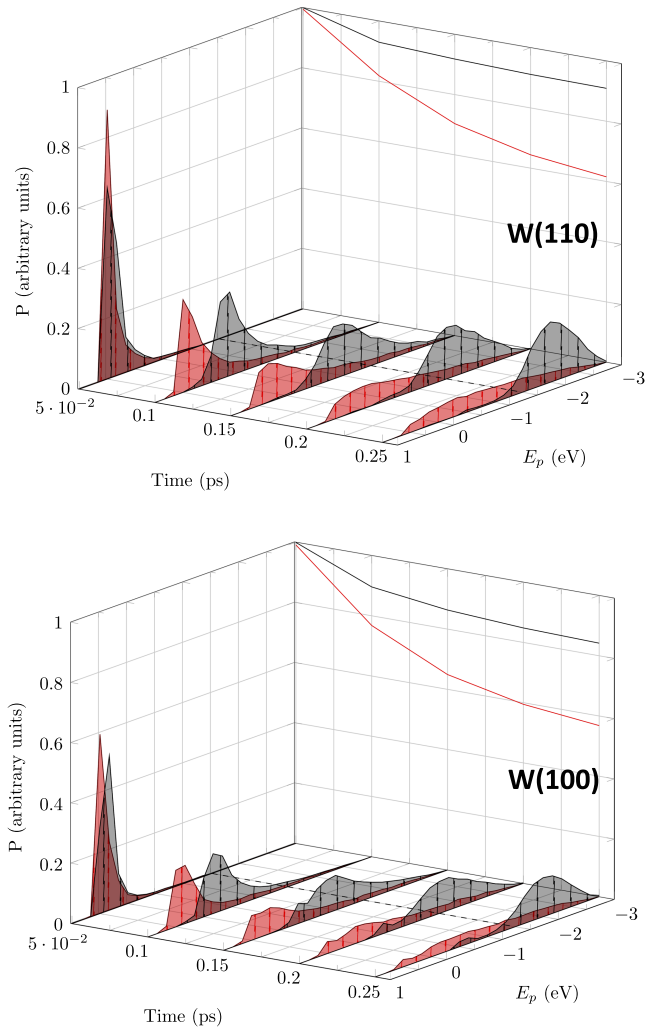

FIG. 3. Total energy distributions of the projectiles travelling at the surface at different times for BOSS (red) and LDFA (black) calculations for E_i = 0.5 eV and θ = 0.25 ML for W(110) (top panel, left front) and θ = 0.5 ML for W(100) (bottom panel, left front). The curves in the right front plane display the fraction of projectiles adsorbed on the surface as a function of time. The dashed line (E_p = 1.5 eV) indicates the threshold energy below which abstraction becomes endothermic.

To conclude, we have theoretically investigated for the first time the effect of surface structure on hot-atom abstraction, with and without including the effect of *e–h* pair excitations, for hydrogen abstraction on W(100) and W(110) surfaces. Electron-hole pair excitations strongly reduce the hot-atom abstraction cross section in favor of H adsorption, but no significant differences are obtained for the two studied surfaces. Thus, a result common to both surfaces, which actually contravenes previous assumptions, is that the Eley-Rideal and hot-atom mechanisms contribute equally to the total H-H abstraction process. Considering that the distinct H-H abstraction dynamics in both crystal faces cover scenarios of different non-adiabatic couplings, this result is most likely generalizable to all metals and crystal faces, at least for exothermic H–H abstraction processes of a few eVs. The reason is that this amount of energy is efficiently dissipated into *e–h* pairs within the sub-picosecond time scale that usually characterizes the fast Eley-Rideal recombination.

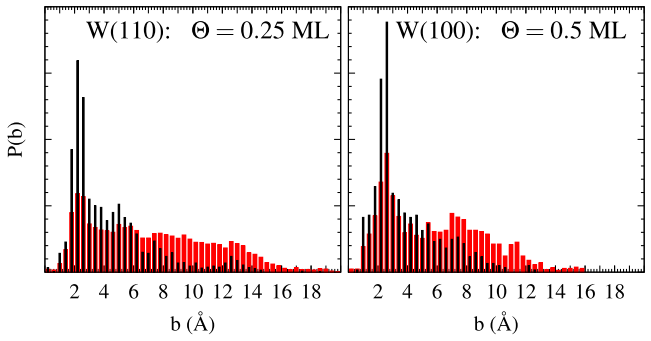

FIG. 4. Normalized travelled distance distribution for abstraction for 0.5 eV incidence energy within the BOSS (red) and LDFA (black) calculations for both W(100) (right) and W(110) (left) surfaces.

O.G., J.I.J., and M.A. acknowledge financial support by the Basque Departamento de Educación, Universidades e Investigación, the University of the Basque Country UPV/EHU (Grant No. IT-756-13), and the Spanish Ministerio de Economía y Competitividad (Grant Nos. FIS2013-48286-C2-2-P and FIS2016-76471-P). O.G., M.A., and P.L. acknowledge the IDEX Bordeaux (No. ANR-10-IDEX-03-02) and Euskampus for funding. Computational resources were provided by the DIPC computing center, the Mésocentre de Calcul Intensif Aquitain (MCIA). France Grilles is also acknowledged for providing computing resources on the French National Grid Research conducted in the scope of the Transnational Common Laboratory "QuantumChemPhys: Theoretical Chemistry and Physics at the Quantum Scale."

[1]R. Díez Muiño and H. Busnengo, *Dynamics of Gas-Surface Interactions: Atomic-level Understanding of Scattering Processes at Surfaces*, Springer Series in Surface Sciences (Springer, 2013).
[2]G. Somerjai, *Introduction to Surface Chemistry and Catalysis* (John Wiley & Sons, 2004).
[3]F. Bozzo, G. Ertl, M. Grunze, and M. Weiss, J. Catal. **50**, 519 (1977).
[4]M. A. Nosir, L. Martin-Gondre, G. A. Bocan, and R. Díez Muiño, Phys. Chem. Chem. Phys. **19**, 7370 (2017).
[5]I. Goikoetxea, M. Alducin, R. Díez Muiño, and J. I. Juaristi, Phys. Chem. Chem. Phys. **14**, 7471 (2012).
[6]I. Goikoetxea, J. I. Juaristi, R. Díez Muiño, and M. Alducin, Phys. Rev. Lett. **113**, 066103 (2014).
[7]H. E. Pfnür, C. T. Rettner, J. Lee, R. J. Madix, and D. J. Auerbach, J. Chem. Phys. **85**, 7452 (1986).
[8]C. T. Rettner, E. K. Schweizer, H. Stein, and D. J. Auerbach, Phys. Rev. Lett. **61**, 986 (1988).
[9]C. T. Rettner, H. Stein, and E. K. Schweizer, J. Chem. Phys. **89**, 3337 (1988).
[10]M. Alducin, R. Díez Muiño, H. F. Busnengo, and A. Salin, Phys. Rev. Lett. **97**, 056102 (2006).
[11]L. Vattuone, M. Rocca, C. Boragno, and U. Valbusa, J. Chem. Phys. **101**, 713 (1994).
[12]F. de Mongeot, M. Rocca, and U. Valbusa, Surf. Sci. **363**, 68 (1996).
[13]A. Raukema, D. A. Butler, F. M. Box, and A. W. Kleyn, Surf. Sci. **347**, 151 (1996).
[14]M. Alducin, H. F. Busnengo, and R. Díez Muiño, J. Chem. Phys. **129**, 224702 (2008).
[15]I. Goikoetxea, J. Beltrán, J. Meyer, J. I. Juaristi, M. Alducin, and K. Reuter, New J. Phys. **14**, 013050 (2012).
[16]I. Lončarić, M. Alducin, and J. I. Juaristi, Phys. Chem. Chem. Phys. **17**, 9436 (2015).
[17]I. Loncaric, M. Alducin, and J. I. Juaristi, Phys. Chem. Chem. Phys. **18**, 27366 (2016).
[18]T. Kammler, J. Lee, and J. Küppers, J. Chem. Phys. **106**, 7362 (1997).
[19]T. Kammler, S. Wehner, and J. Küppers, J. Chem. Phys. **109**, 4071 (1998).
[20]S. Wehner and J. Küppers, J. Chem. Phys. **108**, 3353 (1998).
[21]S. Wehner and J. Küppers, Surf. Sci. **411**, 46 (1998).
[22]T. Zecho, B. Brandner, and J. Küppers, Surf. Sci. Lett. **418**, L26 (1998).
[23]T. Kammler and J. Küppers, J. Chem. Phys. **111**, 8115 (1999).

[24]D. Kolovos-Vellianitis, T. Kammler, and J. Küppers, Surf. Sci. **454-456**, 316 (2000).
[25]D. Kolovos-Vellianitis and J. Küppers, Surf. Sci. **548**, 67 (2004).
[26]G. E. Eilmsteiner, W. Walkner, and A. Winkler, Surf. Sci. **352-354**, 263 (1996).
[27]G. E. Eilmsteiner and A. Winkler, Surf. Sci. **366**, L750 (1996).
[28]J. Boh, G. E. Eilmsteiner, K. D. Rendulic, and A. Winkler, Surf. Sci. **395**, 98 (1998).
[29]H. Poelzl, G. Strohmmeier, and A. Winkler, J. Chem. Phys. **110**, 1154 (1999).
[30]D. D. Eley and E. K. Rideal, Nature **146**, 401 (1940).
[31]J. Harris and B. Kasemo, Surf. Sci. **105**, L281 (1981).
[32]E. Quintas-Sánchez, P. Larrégaray, C. Crespos, L. Martin-Gondre, J. Rubayo-Soneira, and J. C. Rayez, J. Chem. Phys. **137**, 064709 (2012).
[33]E. Quintas-Sánchez, C. Crespos, P. Larrégaray, J. C. Rayez, L. Martin-Gondre, and J. Rubayo-Soneira, J. Chem. Phys. **138**, 024706 (2013).
[34]E. Quintas-Sánchez, P. Larrégaray, and C. Crespos, J. Phys. Chem. C **118**, 12224 (2014).
[35]R. Pétuya, C. Crespos, E. Quintas-Sánchez, and P. Larrégaray, J. Phys. Chem. C **118**, 11704 (2014).
[36]R. Pétuya, P. Larrégaray, C. Crespos, H. F. Busnengo, and A. E. Martínez, J. Chem. Phys. **141**, 024701 (2014).
[37]O. Galparsoro, R. Pétuya, J. I. Juaristi, C. Crespos, M. Alducin, and P. Larrégaray, J. Phys. Chem. C **119**, 15434 (2015).
[38]D. V. Shalashilin and B. Jackson, J. Chem. Phys. **109**, 2856 (1998).
[39]D. V. Shalashilin, B. Jackson, and M. Persson, J. Chem. Phys. **110**, 11038 (1999).
[40]Z. B. Guvenc, X. Sha, and B. Jackson, J. Phys. Chem. B **106**, 8342 (2002).
[41]J. Y. Kim and J. Lee, J. Chem. Phys. **113**, 2856 (2000).
[42]B. Jackson, X. Sha, and Z. B. Guvenc, J. Chem. Phys. **116**, 2599 (2002).
[43]R. Pétuya, P. Larrégaray, C. Crespos, P. Aurel, H. F. Busnengo, and A. E. Martínez, J. Phys. Chem. C **119**, 3171 (2015).
[44]O. Galparsoro, R. Pétuya, F. Busnengo, J. I. Juaristi, C. Crespos, M. Alducin, and P. Larregaray, Phys. Chem. Chem. phys. **18**, 31378 (2016).
[45]M. Pavanello, D. J. Auerbach, A. M. Wodtke, M. Blanco-Rey, M. Alducin, and G.-J. Kroes, J. Phys. Chem. Lett. **4**, 3735 (2013).
[46]M. Blanco-Rey, J. I. Juaristi, R. Díez Muiño, H. F. Busnengo, G. J. Kroes, and M. Alducin, Phys. Rev. Lett. **112**, 103203 (2014).
[47]G.-J. Kroes, M. Pavanello, M. Blanco-Rey, M. Alducin, and D. J. Auerbach, J. Chem. Phys. **141**, 054705 (2014).
[48]D. Novko, M. Blanco-Rey, J. I. Juaristi, and M. Alducin, Phys. Rev. B **92**, 201411 (2015).
[49]D. Novko, M. Blanco-Rey, J. Juaristi, and M. Alducin, Nucl. Instrum. Methods Phys. Res., Sect. B **382**, 26 (2016).
[50]D. Novko, M. Blanco-Rey, J. I. Juaristi, and M. Alducin, Phys. Rev. B **93**, 245435 (2016).
[51]O. Bünermann, H. Jiang, Y. Dorenkamp, A. Kandratsenka, S. M. Janke, D. J. Auerbach, and A. M. Wodtke, Science **350**, 1346 (2015).
[52]A. Wodtke, Chem. Soc. Rev. **45**, 3641 (2016).
[53]O. Galparsoro, F. Busnengo, J. I. Juaristi, C. Crespos, M. Alducin, and P. Larregaray, "Energy dissipation to tungsten surfaces upon hot-atom and Eley-Rideal recombination of H2 from W100" (unpublished).
[54]H. Busnengo, A. Salin, and W. Dong, J. Chem. Phys. **112**, 7641 (2000).
[55]R. A. Olsen, H. F. Busnengo, A. Salin, M. F. Somers, G. J. Kroes, and E. J. Baerends, J. Chem. Phys. **116**, 3841 (2002).
[56]G. Kresse, Phys. Rev. B **62**, 8295 (2000).
[57]L. Bonnet and J.-C. Rayez, Chem. Phys. Lett. **277**, 183 (1997).
[58]L. Bonnet, J. Chem. Phys. **133**, 174108 (2010).
[59]L. Bonnet, Int. Rev. Phys. Chem. **32**, 171 (2013).
[60]J. I. Juaristi, M. Alducin, R. Díez Muiño, H. F. Busnengo, and A. Salin, Phys. Rev. Lett. **100**, 116102 (2008).
[61]I. Goikoetxea, J. I. Juaristi, M. Alducin, and R. Díez Muiño, J. Phys.: Condens. Matter **21**, 264007 (2009).
[62]L. Martin-Gondre, G. A. Bocan, M. Alducin, J. I. Juaristi, and R. Díez Muiño, Comput. Theor. Chem. **990**, 126 (2012).
[63]L. Martin-Gondre, M. Alducin, G. A. Bocan, R. Díez Muiño, and J. I. Juaristi, Phys. Rev. Lett. **108**, 096101 (2012).
[64]J. C. Tremblay, S. Monturet, and P. Saalfrank, Phys. Rev. B **81**, 125408 (2010).
[65]G. Füchsel, T. Klamroth, S. Monturet, and P. Saalfrank, Phys. Chem. Chem. Phys. **13**, 8659 (2011).
[66]J. I. Juaristi, M. Alducin, and P. Saalfrank, Phys. Rev. B **95**, 125439 (2017).
[67]R. Martinazzo, S. Assoni, G. Marinoni, and G. F. Tantardini, J. Chem. Phys. **120**, 8761 (2004).